Lattice QCD thermodynamics from cumulants of conserved charge fluctuations

Dennis Bollweg[1] for the HotQCD Collaboration

CIPANP 2022

[1]Brookhaven National Lab

Lake Buena Vista, 09/01/2022

Based on [Phys.Rev.D 105 (2022) 7, 074511] and [Phys.Rev.D 104 (2021) 7, 074512]

Outline

Motivation

- Exploration of QCD phase diagram poses long-standing open challenge in HIC research.
- $T_{pc} = 156.5(1.5)$ MeV and $T_c = 132^{+3}_{-6}$ MeV established in lattice calculations [arXiv:1812:08235], [arXiv:1903:04801].
- Discovery of critical endpoint (CEP) still outstanding.
- Bulk thermodynamic properties (Pressure P, energy density ϵ, number densities $n, \ldots$) of QCD are needed inputs for wide range of phenomena (HIC, early universe, compact stars, ...)
- Hadron resonance gas models widely used in phenomenological applications but which spectrum to use?

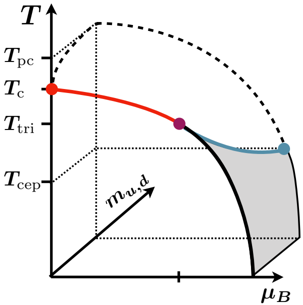

Cumulants of conserved charge fluctuations χ^{BQS}_{ijk} calculated via lattice QCD help addressing all of these points.

Generalized Susceptibilities via lattice QCD

$$\chi_{ijk}^{BQS} \equiv \frac{1}{VT^3} \frac{\partial^{i+j+k} \log \mathcal{Z}}{\partial \hat{\mu}_B^i \partial \hat{\mu}_Q^j \partial \hat{\mu}_S^k}, \quad \hat{\mu}_X \equiv \frac{\mu_X}{T}$$

To compute χ_{ijk}^{BQS}, we need to solve integrals of the form

$$\frac{1}{\mathcal{Z}} \int \prod_{x,\nu} \mathrm{d}U_{x,\nu} \mathrm{Tr}\left(M_f^{-1} M'_f \cdots \right) \mathrm{e}^{-S_{\mathrm{eff}}}.$$

These are calculated via Markov-Chain Monte-Carlo:

1. Generate $\{U_{x,\nu}\}$-ensembles via RHMC algorithm[1].
2. Evaluate $\mathrm{Tr}\left(M_f^{-1} M'_f \cdots \right)$ on $\{U_{x,\nu}\}$-ensembles using random noise method: $\mathrm{Tr}\left(\hat{\mathcal{M}}_f\right) \sim \frac{1}{N} \sum_{i=0}^{N} \eta_i^* \hat{M}_f \eta_i$. → Sparse matrix inversions with 500-2000 right-hand sides η_i for each trace.

[1] https://github.com/LatticeQCD/SIMULATeQCD

HotQCD Setup & Statistics

- Dynamical Fermions (HISQ) with $N_f = 2+1$, physical quark masses ($\frac{m_s}{m_l} = 27$), $T \in [135, 175]$ MeV and lattice sizes $N_\tau = 6, 8, 12, 16$, $N_\sigma = 4N_\tau$.
- Up to 8th order χ^{BQS}_{ijk} $(i+j+k \leq 8)$ available.
- For Temperatures $T > 180$ MeV: $\frac{m_s}{m_l} = 20$ and $N_\tau = 6, 8, 12$[2].

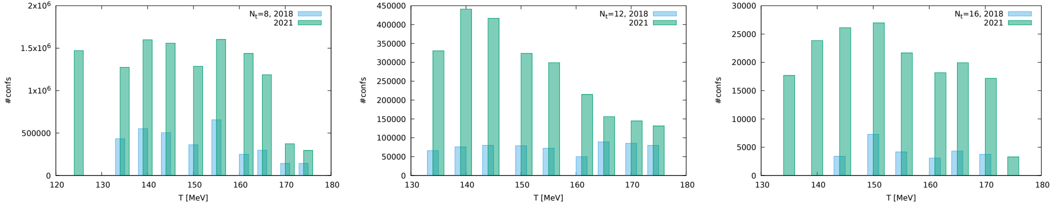

Data set 2022 [arXiv:2202.09184] vs 2017 [arxiv:1701.04325]

[2]Only lowest orders available for $N_\tau = 12$ at $T > 180$ MeV

LQCD and Hadron Resonance Gas

- QCD describes the dynamics of strongly interacting matter both in the high and low temperature regime.
- Hadron resonance gas (HRG) models are used to describe the low temperature regime of QCD and find wide phenomenological application, for example in the extraction of freeze-out parameters in HIC experiments.
- HRG models are in quite good agreement with the lowest order cumulants (χ_n^X) calculated in Lattice QCD at $T < T_{pc}$, however more quantitative agreement depends on details of the hadron resonance spectrum and the treatment of interactions.
- Agreement starts to deteriorate as T approaches T_{pc}.

Non-interacting HRG

Pressure in a non-interacting HRG reads,

$$P/T^4 = \sum_H \frac{g}{2\pi^2} \left(m_H/T\right)^2 \sum_{k=1}^{\infty} \frac{(\pm)^{k+1}}{k^2} K_2\left(\frac{km_H}{T}\right) \exp\left[k\vec{C}_H \cdot \vec{\mu}/T\right]$$

$$\vec{\mu} = \left(\mu_B, \mu_Q, \mu_S\right), \quad \vec{C}_H = \left(B_H, Q_H, S_H\right).$$

Susceptibilities are given by,

$$\chi_{ijk}^{BQS} \propto \sum_H B_H^i Q_H^j S_H^k P_H .$$

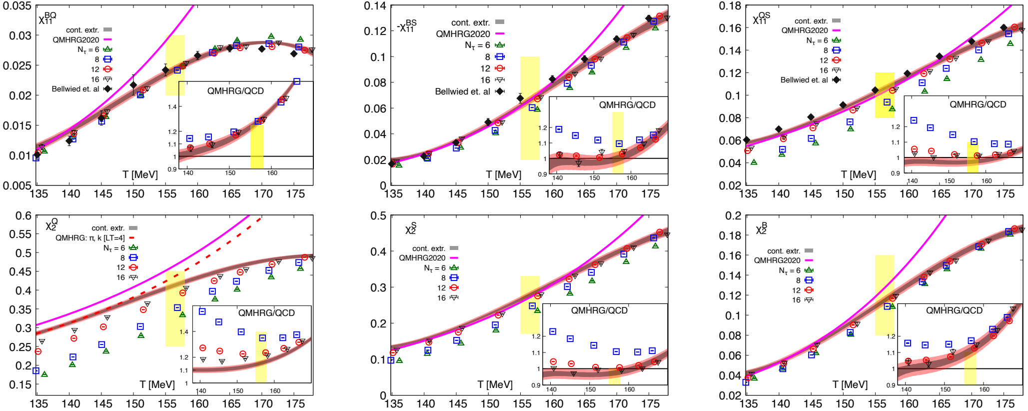

Figure: Continuum extrapolations of second order susceptibilities vs. QM-HRG2020.

[Phys. Rev. D 104 (2021) 074512]

QMHRG vs. PDG-HRG

- **PDG-HRG**: established resonances from PDG2020 (3 and 4 star).
- **QM-HRG**: 1 and 2 star resonances from PDG2020 and additional states from Quark Model calculations.
- PDG-HRG fails to describe baryon-strangeness correlation (χ_{11}^{BS}), whereas QMHRG works for $T \leq T_{pc} = 156.5(1.5)$ MeV.
- QM-HRG baryon-electric charge correlations (χ_{11}^{BQ}) deviate by 50% from lattice QCD results.
- Treating hadronic system near T_{pc} via non-interacting, point-like resonances is not sufficient!

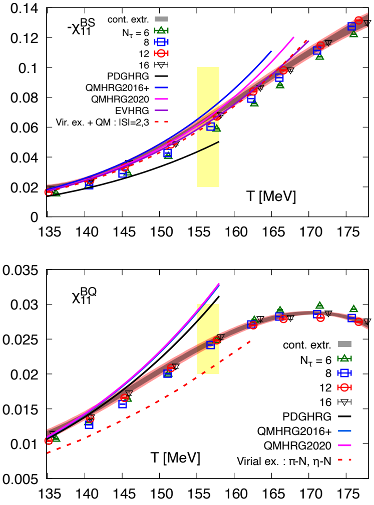

Excluded Volume HRG models

- LQCD and HRG model calculations start to deviate close to $T \sim T_{pc}$ using only non-interacting hadronic resonances because of the exponentially rising nature of HRG.
- Natural extension: Introducing additional repulsive interaction through Excluded Volume HRG. EV parameter b is introduced to match lattice data.
- Change in 2nd order cumulants involving baryon-number, calculated in EV-HRG and HRG models, is identical.

$$R_B^{EV} = \frac{(\chi_{11}^{BQ})_{\rm EVHRG}}{(\chi_{11}^{BQ})_{\rm HRG}} = \frac{(\chi_{11}^{BS})_{\rm EVHRG}}{(\chi_{11}^{BS})_{\rm HRG}} = \ldots$$
$$= 1 - 2\frac{b}{T} P_B^{\rm HRG}(T) + \mathcal{O}(b^2).$$

[Phys. Rev. C 100, 065202 (2019)]

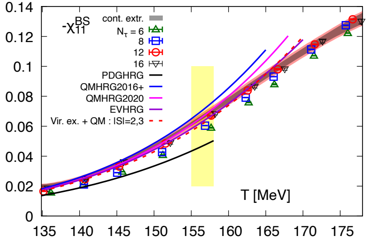

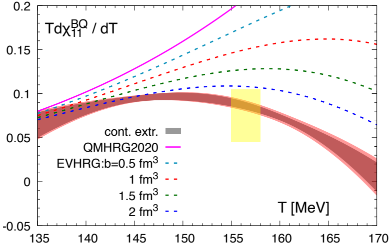

Excluded Volume HRG models

- Calculate maximal (minimal) b necessary to match lattice results

$$b^{\pm} = \frac{1}{2T^3(\chi_2^B)_{\mathrm{HRG}}}\left(1 - \frac{(\chi_{11}^{BX} \pm \Delta_X)_{\mathrm{QCD}}}{(\chi_{11}^{BX})_{\mathrm{HRG}}}\right).$$

- **No choice of b results in EV-HRG matching χ_{11}^{BS} and χ_{11}^{BQ} simultaneously!**
- χ_{11}^{BS} requires $b < 0.4$ fm whereas χ_{11}^{BQ} requires $1\ \mathrm{fm} \leq b \leq 2$ fm to be consistent with lattice results.
- Proper treatment of attractive interactions in diff. quantum channels is needed! (Ex. Virial Expansions/S-matrix HRG approaches [Phys. Rev. C 96, 015207]).

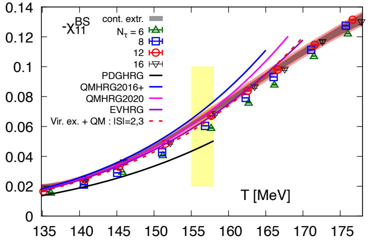

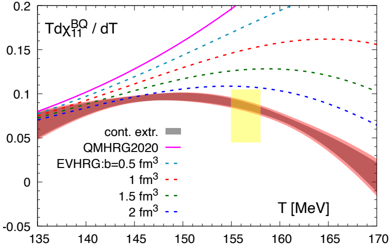

Equation of State via Taylor expansion

Expansion of the QCD pressure in μ/T:

$$\frac{P(T,\mu)}{T^4} = \sum_{i,j,k=0} \frac{\chi_{ijk}^{BQS}(T)}{i!j!k!} \hat{\mu}_B^i \hat{\mu}_Q^j \hat{\mu}_S^k, \quad \hat{\mu}_x = \frac{\mu_x}{T},$$

$$\chi_{ijk}^{BQS}(T) = \frac{1}{VT^3} \left. \frac{\partial^{i+j+k} \ln \mathcal{Z}}{\partial \hat{\mu}_B^i \partial \hat{\mu}_Q^j \partial \hat{\mu}_S^k} \right|_{\vec{\mu}=0} .$$

Constraints on expansion are imposed depending on application
Popular choices include:

- $\mu_Q = \mu_S = 0$
- Heavy Ion Collision conditions: $n_Q/n_B = 0.4,\ n_S = 0 \rightarrow \mu_S(\mu_B),\ \mu_Q(\mu_B)$
- Isospin symmetric: $n_Q/n_B = 0.5,\ n_S = 0 \rightarrow \mu_S(\mu_B),\ \mu_Q = 0.$

Expansion coefficients of the QCD pressure

Constrained expansion of the QCD pressure: $(P(T,\mu_B) - P(T,0))/T^4 = \sum_k (\bar{\chi}_0^{B,2k}/2k!)\hat{\mu}_B^{2k} = \sum_k P_{2k}\hat{\mu}_B^{2k}$

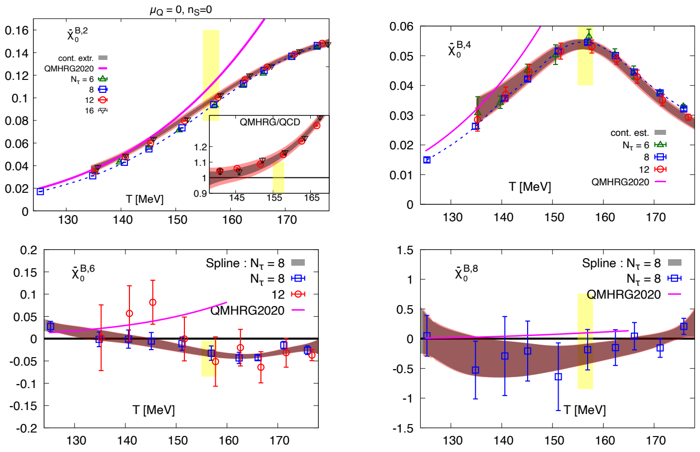

- Continuum extrapolated results for 2nd and 4th order based on $N_\tau \in \{6, 8, 12, 16\}$ and $N_\tau \in \{6, 8, 12\}$ lattices, respectively.
- Spline interpolation based on $N_\tau = 8$ lattices for 6th and 8th order.
- Deviations from HRG rapidly increase with increasing order.

Equation of State via Taylor expansion

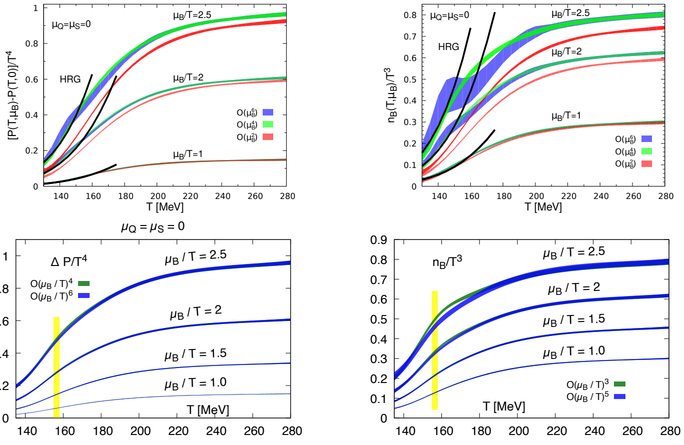

EoS 2017 (top) vs 2022 (bottom)

- Better control over $\mathcal{O}(\mu_B^6)$ significantly reduces "wiggles" at high μ_B/T.

Equation of State up to 8th order

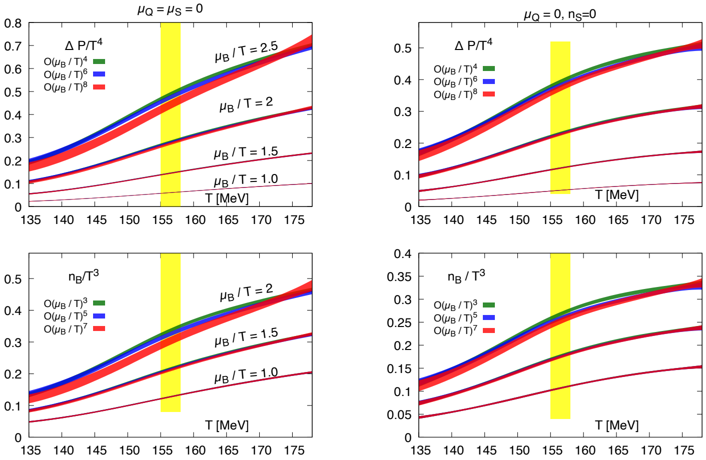

Radius and rate of convergence

- Radius of convergence r_c of $f(x) = \sum_n c_n x^n$ is given by closest singularity in complex x-plane.
- Rate of convergence/reliability of series judged by agreement of subsequent orders.
- Pressure, Baryon number density n_B, χ_2^B, ... share same r_c but rate of convergence varies.

Simple estimator $r_{c,n}$ for radius of convergence given by

$$r_c = \lim_{n\to\infty} r_{c,n} = \lim_{n\to\infty} \sqrt{\frac{|c_n|}{|c_{n+2}|}}.$$

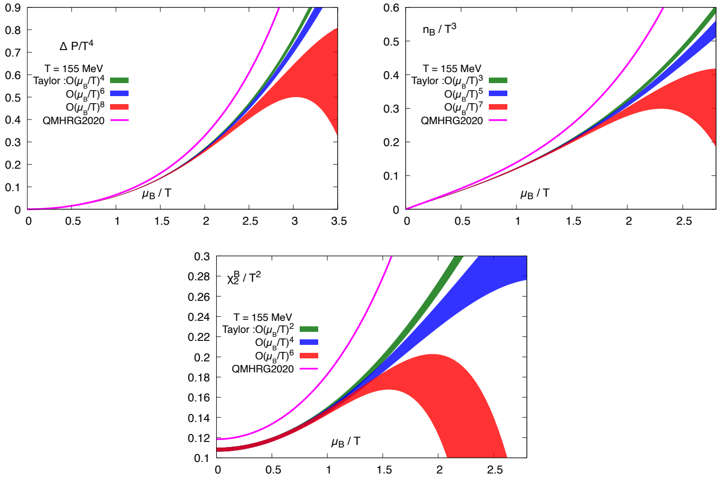

- Agreement of subsequent orders shifts to smaller μ_B/T for higher order cumulants.
- 8th order Taylor expansions for P, n_B and χ_2^B reliable up to $\mu_B/T \sim 2.5, 2$ and 1.5, respectively.

Padé approximants

- Within $|\hat{\mu}_B| < r_c$, Taylor expansion can be improved by incorporating higher orders but method fails beyond $|\hat{\mu}_B| = r_c$.
- Phase transitions are related to singularities of $\log Z$ on the real axis.
- Padé approximants converge beyond closest singularity.

$$[m,n]_f(x) = \frac{\sum_{i=0}^{m} a_i x^i}{\sum_{j=0}^{n} b_j x^j} \quad \text{with} \quad [m,n]_f(0) = f(0), \ldots, [m,n]^{(m+n)}(0) = f^{(m+n)}(0),$$

- Poles of Padé approximants closest to origin determine radius of convergence: Poles of $[m,2]$ and $[n,4]$ Padés reproduce standard estimator $r_{c,n}$ and Mercer Roberts estimator:

$$r_{c,n} = \sqrt{\frac{|c_n|}{|c_{n+2}|}}, \quad r_{c,n}^{MR} = \left| \frac{c_{n+2}c_{n-2} - c_n^2}{c_{n+4}c_n - c_{n+2}^2} \right|^{1/4}$$

Padé approximants: Location of poles

[4,4] Pade approximant for the pressure:

$$P[4,4] = \frac{(1-c_{6,2})\bar{x}^2 + (1-2c_{6,2}+c_{8,2})\bar{x}^4}{(1-c_{6,2}) + (c_{8,2}-c_{6,2})\bar{x}^2 + (c_{6,2}^2 - c_{8,2})\bar{x}^4}, \quad \text{with} \quad \bar{x} = \sqrt{\frac{P_4}{P_2}}\hat{\mu}_B, \quad c_{2k,2} = \frac{P_{2k}}{P_2}\frac{P_2}{P_4}^{k-1}$$

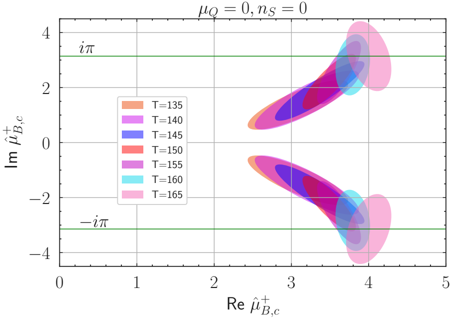

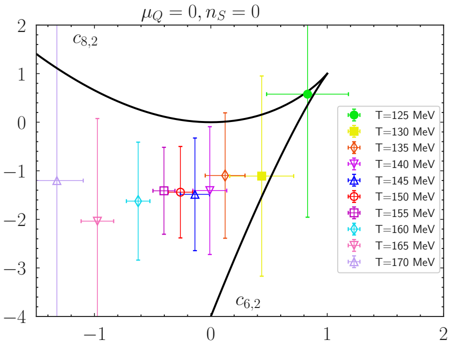

Left: Position of poles with pos. real part. Poles move towards real axis with decreasing T. Right: Condition for appearance of real poles. Real poles cannot be ruled out for $T < 135$ MeV!

Padé approximants: Radius of convergence

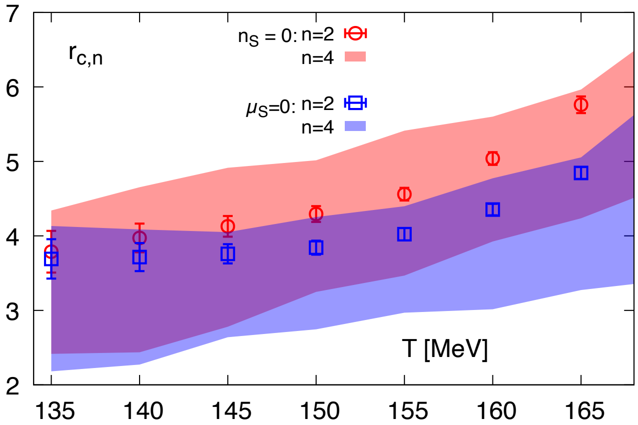

Distance of poles of the [2,2] and [4,4] Padé approximants from the origin as a function of T.

Summary

- Multi-year computation campaign generating high statistics data set of (2+1)-flavor HISQ configurations.
- Precise calculation of 2nd order cumulants and correlations of conserved charge fluctuations which allows to constrain HRG models.
- Extension of Equation of State Taylor expansion coefficients up to 8th order.
- 8th order Taylor expansions for P, n_B and χ_2^B reliable up to $\mu_B/T \sim 2.5, 2$ and 1.5, respectively.
- Poles of Padé approximants of QCD pressure consistent with absence of CEP for $T > 135$ MeV and $\mu_B/T < 2.5$.